A copper complex bearing a TEMPO moiety as catalyst for the aerobic oxidation of primary alcohols†

Zhengliang Lu,[a] José Sánchez Costa,[a] Olivier Roubeau,[b] Ilpo Mutikainen,[c] Urho Turpeinen,[c] Simon J. Teat,[d] Patrick Gamez*[a] and Jan Reedijk*[a]

Received 6th February 2008, Accepted 11th April 2008
First published as an Advance Article on the web 7th May 2008
DOI: 10.1039/b802109k

A new bifunctional, triazine-based ligand has been designed with the aim to generate a copper(II) complex holding a TEMPO (2,2,6,6-tetramethylpiperidinyloxy) moiety. The coordination compound obtained from the ligand 4-(2-(3-(pyridin-2-yl)-1*H*-pyrazol-1-yl)ethoxy)-6-(4-amino-2,2,6,6-tetramethylpiperidine-1-oxyl)-*N*,*N*-diphenyl-1,3,5-triazin-2-amine (pypzt-1) and copper(II) bromide (*i.e.* complex **8**) is capable of catalysing the selective, aerobic oxidation of benzyl alcohol to 84% of benzaldehyde in 24 h. This "galactose oxidase activity" of the copper/TEMPO complex is observed as well for the conversion of the non-activated alkyl alcohol octan-1-ol to octanal with a yield of 29% after the same reaction time. The single-crystal X-ray structure of **8** shows that its crystal lattice contains $[Cu^{I}Br_2]^-$ anions which appear to be stabilised by means of both anion–π and hydrogen bonding interactions. In addition, the solid state structure of **8** exhibits (lone-pair)–π interactions between the nitrogen atom of an acetonitrile molecule and a triazine ring. The magnetic properties of **8** have been investigated by EPR and magnetic susceptibility measurements.

Introduction

The selective oxidation of alcohols is an important synthetic transformation in organic chemistry.[1,2] In particular, the production of aldehydes from primary alcohols represents one of the most critical challenges facing the chemical industry.[3] Different methods have been developed to achieve this chemical conversion. For instance, an aldehyde is typically obtained by reaction of an alcohol with a chromium(VI) reagent which is reduced to Cr^{3+} during the reaction. However, most of these oxidation procedures involve the use of stoichiometric amounts of toxic salts.[4,5] Therefore, the development of selective and environmentally friendly oxidations catalysed by transition-metal complexes is a very important and topical area of contemporary catalysis.[6] Several catalytic procedures have been described,[7,8] but some limitations remain that are the chemo-, regio- and stereoselectivity of the procedures. TEMPO-based (TEMPO stands for 2,2,6,6-tetramethylpiperidinyloxy) systems have shown great potential as environmentally benign alternatives to oxidations where copious amounts of ecologically unfriendly metal salts are used.[9–15] Especially, a number of [copper/TEMPO] catalysts have proven to be highly efficient and versatile systems for the production of a broad range of aldehydes.[16–23]

A few years ago, some of us have reported a [copper(2,2′-bipyridine)/TEMPO]-based catalyst capable of selectively converting primary alcohols to the corresponding aldehydes at room temperature.[24,25] Recently, this efficient catalytic system with bipyridine ligands has been extended to the use of mixed pyrazole/pyridine ligands.[26] The oxidation procedure brings in the [copper/ligand] catalyst obtained *in situ* and the TEMPO co-catalyst as single reagents.[25] In the present study, two new ligands containing one pyrazole and one pyridine donors and holding a TEMPO moiety have been designed and synthesized. These bifunctional molecules including both catalyst precursors, *i.e.* the ligand to coordinate copper(II) ions and the radical unit, are tested for the aerobic oxidation of primary alcohols to the corresponding aldehydic products.

Experimental

General

All chemicals were used as obtained without further purification. ^{1}H and ^{13}C NMR spectra were recorded using a DPX 300 Bruker (300 MHz) instrument. Chemical shifts are reported in ppm (parts per million) relative to the solvent peak. Elemental analyses (C, H, N) were carried out on a Perkin-Elmer 2400 series II analyzer. FTIR spectra were recorded with a Perkin-Elmer Paragon 1000 FTIR spectrophotometer, equipped with a Golden Gate ATR device, using the reflectance technique (4000-300 cm^{-1}). ESI mass analyses were carried out on a Voyager Elite from PerSeptive Biosystems. X-Band electron paramagnetic resonance (EPR) measurements were performed on a Bruker EMX spectrometer. Magnetic susceptibility measurements (5–300 K) were carried out

[a]*Leiden Institute of Chemistry, Leiden University, P.O. Box 9502, 2300, RA, Leiden, The Netherlands. E-mail: reedijk@chem.leidenuniv.nl; Fax: +31 715274671*
[b]*Université Bordeaux 1, CNRS-CRPP, 115 avenue du dr. A. Schweitzer, 33600, Pessac, France*
[c]*University of Helsinki, Department of Chemistry, Laboratory of Inorganic Chemistry, Helsinki, 00014, Finland*
[d]*ALS, Berkeley Lab, 1 Cyclotron Road, MS2-400, Berkeley, CA, 94720, USA*

† Electronic supplementary information (ESI) available: X-Ray data for compounds **6a** and **6b** (Table S1), **7a** and **7b** (Table S2) and their X-ray structure representations (Figs. S1–S4); contact distances characterising the anion–π (Table S3) and the lone pair–π (Table S4) interactions. CCDC reference numbers 676753–6767657 (**6a**, **6b**, **7a**, **7b** and **8**). For ESI and crystallographic data in CIF or other electronic format see DOI: 10.1039/b802109k

using a Quantum Design MPMS-5S SQUID magnetometer at 1000 Oe. Data were corrected for the diamagnetic contributions estimated from the Pascal constants.[27]

Syntheses

Synthesis of the TEMPO-containing ligands pypzt-1 and pypzt-2 and their precursors

2,4-Dichloro-6-diphenylamino{1,3,5}triazine (2). **2** was prepared from 2,4,6-trichloro-1,3,5-triazine (**1**) and diphenylamine applying a synthetic procedure described earlier.[28]

3-(Dimethylamino)-1-(pyridin-2-yl)prop-2-en-1-one (4). **4** was synthesized by reaction of 2-acetylpyridine (**3**) with *N*,*N*-dimethylformamide dimethyl acetal, following a procedure used to prepare a related compound.[29] 10 g (82.5 mmol) of 2-acetylpyridine (**3**) were introduced in a round-bottomed flask. Then, 18.5 g (155 mmol) of *N*,*N*-dimethylformamide dimethyl acetal were added and the resulting reaction mixture was refluxed overnight. The dark solution obtained was evaporated to dryness under reduced pressure. Dark brown crystals of **4**[26] (3.62 g, 33 mmol; yield = 40%) were obtained and washed with hexane (3 × 100 mL) and with diethyl ether (3 × 100 mL). The ^{1}H NMR spectrum of compound **4** is identical to that earlier reported.[26]

2-(3-(Pyridin-2-yl)-1*H*-pyrazol-1-yl)ethanol (5a) and 2-(5-(pyridin-2-yl)-1*H*-pyrazol-1-yl) ethanol (5b). 2 g (11.3 mmol) of **4** and 0.912 g (12 mmol) of 2-hydroxyethyl hydrazine were mixed in a 50 mL round-bottomed flask containing 4 mL of ethanol. The red reaction mixture was heated to 60 °C and stirred for 1 h. After cooling to room temperature, the resulting crude orange oil was purified by column chromatography on silica gel. 0.42 g (2.2 mmol, yield = 20%) of **5a** and 1.36 g (7.2 mmol; yield = 63%) of **5b** were collected as orange viscous oils.

Data for 5a. ^{1}H NMR (300 MHz, $CDCl_3$): δ 8.60 (d, 1 H, J = 4.8 Hz), 7.90 (d, 1 H, J = 7.9 Hz), 7.70 (ddd, 1 H, J = 1,7, 7.7 and 7.8 Hz), 7.49 (d, 1 H, J = 2.3 Hz), 7.10 (ddd, 1 H, J = 1.4, 5.0 and 7.0 Hz), 6.88 (d, 1 H, J = 2.3 Hz), 4.30 (t, 2 H, J = 4.5 Hz), 4.05 (t, 2 H, J = 5.0 Hz) ppm; ^{13}C NMR (75 MHz, $CDCl_3$) δ 151.8, 151.5, 149.0, 136.6, 131.7, 122.3, 120.0, 104.1, 61.3, 54.2 ppm. MS-EI$^+$ (m/z) [M]$^{+\bullet}$ 189.95 (calc. 189.21).

Data for 5b. ^{1}H NMR (300 MHz, $CDCl_3$): δ 8.61 (d, 1 H, J = 4.9 Hz), 7.81 (ddd, 1 H, J = 1,6, 7.8 and 7.8 Hz), 7.62 (d, 1 H, J = 7.9 Hz), 7.58 (d, 1 H, J = 1.8 Hz), 7.32 (ddd, 1 H, J = 1.0, 5.0 and 7.5 Hz), 6.57 (d, 1H, J = 1.9 Hz), 4.66 (t, 2 H, J = 4.7 Hz), 4.13 (t, 2 H, J = 4.8 Hz) ppm; ^{13}C NMR (75 MHz, $CDCl_3$) δ 148.2, 147.7, 140.8, 137.9, 136.9, 136.5, 122.8, 122.2, 106.0, 61.5, 51.9 ppm. MS-EI$^+$ (m/z) [M]$^{+\bullet}$ 189.97 (calc. 189.21).

4-(2-(3-(Pyridin-2-yl)-1*H*-pyrazol-1-yl)ethoxy)-6-chloro-*N*,*N*-diphenyl-1,3,5-triazin-2-amine (6a). A solution of **5a** (0.378 g, 2.0 mmol) in 4 mL of dried THF was added dropwise to a suspension of NaH (0.16 g, 60% dispersion in mineral oil; 4 mmol) in 10 mL of dried THF. The resulting suspension was added slowly to a solution of **2** (0.666 g, 2.1 mmol) in 20 mL of THF under stirring. After completion of the addition, the reaction mixture was stirred overnight at room temperature. The reaction mixture was subsequently diluted with a saturated aqueous solution of NaCl and the water layer was extracted three times with EtOAc. The combined organic layer was dried over $MgSO_4$ and the solvent was evaporated under reduced pressure. The residue was purified by column chromatography to obtain compound **6a** as a colourless solid with a yield of 85% (0.797 g, 1.7 mmol).

$C_{25}H_{20}ClN_7O$ (469.93): calc. C 63.90, H 4.29, N 20.86; found C 64.26, H 4.26, N 20.55%. ^{1}H NMR (300 MHz, $CDCl_3$): δ 8.63 (d, 1 H, J = 4.8 Hz), 7.85 (d, 1 H, J = 7.9 Hz), 7.71 (ddd, 1 H, J = 1,5, 7.7 and 7.8 Hz), 7.44–7.17 (m, 12 H), 6.82 (d, 1 H, J = 2 Hz), 4.52 (t, 2 H, J = 5.0 Hz), 4.43 (t, 2 H, J = 5.0 Hz) ppm; ^{13}C NMR (75 MHz, $CDCl_3$) δ 171.3, 170.1, 166.7, 152.0, 149.5, 142.1, 141.6, 136.5, 131.8, 129.2, 127.4, 127.1, 122.4, 120.0, 104.6, 66.6, 50.9 ppm. MS-EI$^+$ (m/z) [M]$^{+\bullet}$ 469.84 (calc. 469.93).

The solid-state structure of **6a** has been determined by single-crystal X-ray diffraction and is depicted in Fig. S1 (ESI†).

4-(2-(5-(Pyridin-2-yl)-1*H*-pyrazol-1-yl)ethoxy)-6-chloro-*N*,*N*-diphenyl-1,3,5-triazin-2-amine (6b). A solution of compound **5b** (0.567 g, 3.0 mmol) in 5 mL of dried THF was added dropwise to a suspension of NaH (0.16 g, 60% dispersion in mineral oil; 4 mmol) in 20 mL of dried THF. The resulting suspension was added dropwise to a solution of **2** in (0.951 g, 3.0 mmol) of 40 mL of THF under stirring. After completion of the addition, the reaction mixture was stirred overnight at room temperature. The reaction mixture was subsequently diluted with a saturated aqueous solution of NaCl and the water layer was extracted three times with EtOAc. The combined organic layer was dried over $MgSO_4$ and the solvent was evaporated under reduced pressure. The residue was purified by column chromatography to obtain compound **6b** as a colourless solid with a yield of 81% (1.13 g, 2.4 mmol).

$C_{25}H_{20}ClN_7O$ (469.93): calc. C 63.90, H 4.29, N 20.86; found C 63.85, H 4.21, N 21.10%. ^{1}H NMR (300 MHz, $CDCl_3$): δ 8.50 (d, 1 H, J = 4.7 Hz), 7.71 (ddd, 1 H, J = 1,6, 7.8 and 7.8 Hz), 7.56 (d, 1 H, J = 7.9 Hz), 7.52 (d, 1 H, J = 1.7 Hz), 7.37 (t, 4 H, J = 7.7 Hz), 7.28–7.18 (m, 7 H), 6.55 (d, 1 H, J = 1.7 Hz), 4.98 (t, 2 H, J = 5.4 Hz), 4.56 (t, 2 H, J = 5.4 Hz) ppm; ^{13}C NMR (75 MHz, $CDCl_3$) δ 171.1, 170.1, 166.7, 149.7, 148.7, 142.3, 141.6, 139.0, 136.8, 129.1, 127.4, 127.0, 123.1, 122.4, 106.8, 67.1, 49.2 ppm. MS-EI$^+$ (m/z) [M]$^{+\bullet}$ 469.94 (calc. 469.93).

The solid-state structure of **6b** has been determined by single-crystal X-ray diffraction and is depicted in Fig. S2 (ESI†).

Ligand pypzt-1 (7a). To a solution of 0.750 g (1.6 mmol) of compound **6a** in 20 mL of THF was added 2 mmol of *N*,*N*-diisopropylethylamine (DiPEA). To this mixture, a solution of 0.31 g (1.8 mmol) of 4-amino-2,2,6,6-tetramethylpiperidine-1-oxyl (4-amino-TEMPO) in 2 mL of THF was added. The resulting orange solution was refluxed for four days. After the reaction mixture was cooled down to room temperature, it was diluted with a saturated aqueous solution of NaCl and the water layer was extracted three times with EtOAc. The combined organic solution was dried over $MgSO_4$ and the solvent was evaporated under reduced pressure. The residue was purified by column chromatography on silica gel to yield pure pypzt-1 (yield = 81%, 0.785 g, 1.3 mmol). $C_{34}H_{38}N_9O_2$ (604.72): calc. C 67.53, H 6.33, N 20.85; found: C 67.46, H 6.38, N 20.35%. MS-EI$^+$ (m/z) [M]$^{+\bullet}$ 603.97 (calc. 604.72).

The solid-state structure of pypzt-1 (**7a**) has been determined by single-crystal X-ray diffraction and is depicted in Fig. S3 (ESI†).

Ligand pypzt-2 (7b). To a solution of 0.938 g (2.0 mmol) of compound **6b** in 20 mL of THF was added 4 mmol (0.660 mL) of DiPEA. To this mixture, a solution of 0.376 g (2.20 mmol) of 4-amino-TEMPO in 4 mL of THF was added. The resulting solution was refluxed for four days after which the mixture was cooled to room temperature. The reaction mixture was subsequently diluted with a saturated aqueous solution of NaCl and the water layer was extracted three times with EtOAc. The combined organic layer was dried over $MgSO_4$ and the solvent was evaporated under reduced pressure. The solid residue was purified by column chromatography on silica gel to produce pypzt-2 with a yield of 80% (0.966 g, 1.6 mmol).

$C_{34}H_{38}N_9O_2$ (604.72): calc. C 67.53, H 6.33, N 20.85; found: C 67.27, H 6.38, N 20.01%. MS-EI$^+$ (m/z) $[M]^{+\bullet}$ 604.93 (calc. 604.72).

The solid-state structure of pypzt-2 (**7b**) has been determined by single-crystal X-ray diffraction and is depicted in Fig. S4 (ESI†).

$[Cu_2(pypzt\text{-}1)_2Br_3(H_2O)][CuBr_2]\cdot 4CH_3CN$ (8). A solution of $CuBr_2$ (16.8 mg, 0.075 mmol) in 4 mL of acetonitrile was added to a stirred solution of TEMPO (31 mg, 0.05 mmol) in 6 mL of acetonitrile. The solution immediately became dark green. After 10 min of stirring, the reaction solution was filtered and the resulting dark-green filtrate was left unperturbed for the slow evaporation of the solvent, at room temperature in air. After two days, dark-orange crystals were obtained which were collected by filtration (yield 35 mg, based on the ligand, 70%).

8 − $4CH_3CN$: calc. C 44.93, H 4.33, N 13.87; found: C 44.69, H 4.45, N 13.07%. IR (neat): ν = 2976, 1584, 1531, 1463, 1441, 1336, 1075, 800, 759, 694, 668, 654, 618, 514, 389 cm^{-1}.

Unfortunately, when this reaction was carried out in the presence of 1 equiv. of base, a precipitate immediately formed.

Typical catalytic experiment. The oxidation of alcohols was carried out in air in a 10 mL round-bottom flask equipped with a magnetic bar. Typically, the alcohols (2.0 mmol) were dissolved in 3 mL of a CH_3CN–H_2O (2 : 1) solvent mixture. 11.2 mg (0.1 mmol) of *tert*-BuOK were added, followed by 22.3 mg (0.1 mmol) of $CuBr_2$, resulting in a blue-green suspension. The ligand (60.4 mg, 0.1 mmol) was added and the reaction suspension slowly turned dark-green. Samples of the reaction mixture were taken out regularly to monitor the reaction by GC.

Structural determinations. Data were collected on an orange block crystal of **8** on station 11.3.1 of the Advanced Light Source synchrotron facility (λ = 0.7749 Å) (for details see ESI†). The structure was solved by direct methods (SHELXS-97)[30] and refined on F^2 (SHELXL-97).[31] Crystal and structure refinement data for **8** are listed in Table 1.

Table 1 Crystal data and structure refinement for $[Cu_2(pypzt\text{-}1)_2Br_3(H_2O)][CuBr_2]\cdot 4CH_3CN$ (**8**)

Formula	$C_{68}H_{78}Br_3Cu_2N_{18}O_5\cdot CuBr_2\cdot 4C_2H_4N$
M_r	1981.87
Crystal size/mm	0.05 × 0.13 × 0.13
T/K	150(2)
Cryst system, space group	Triclinic, $P\bar{1}$ (no. 2)
Crystal colour	Orange
a/Å	14.117(2)
b/Å	17.197(2)
c/Å	19.668(2)
α/°	70.01(2)
β/°	77.21(2)
γ/°	75.18(2)
V/Å^3	4290.4(8)
Z	2
D_c/g cm^{-3}	1.534
$F(000)$	2004
μ/mm^{-1}	4.408
θ for data collection/°	2.73–28.41
Rflns collected (R_{int})	46705 (0.0425)
Data/params	17521/1010
Goodness of fit on F^2	1.035
$R1$ ($wR2$) [$I > 2\sigma(I)$]	0.0668 (0.1712)
$R1$ ($wR2$) (all data)	0.1037 (0.1896)
$\Delta\rho$/e Å^{-3}	1.67 and −1.34

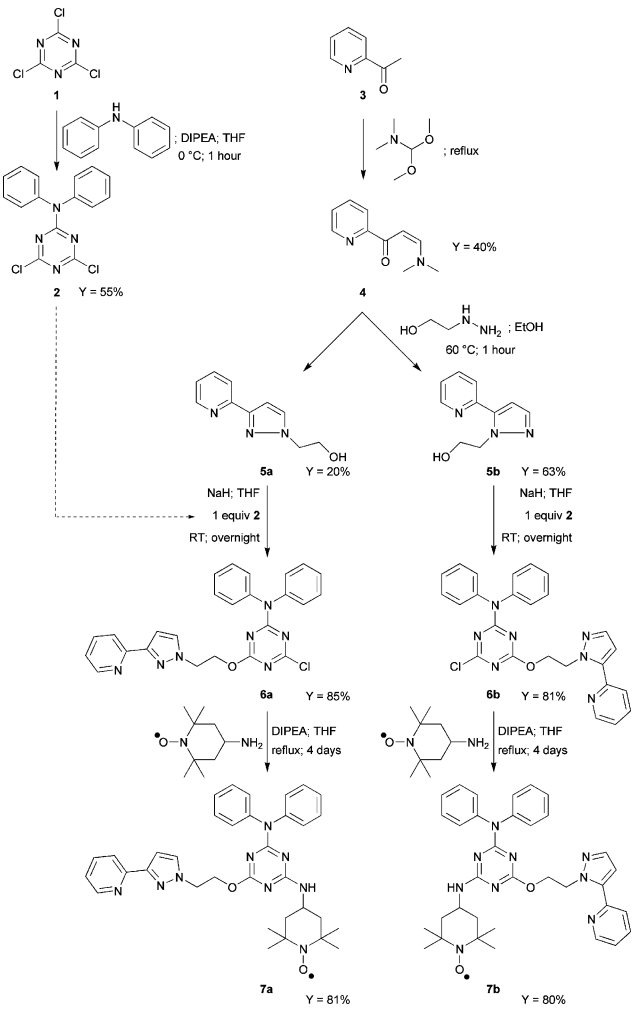

Scheme 1 Synthetic pathway for the preparation of ligands pypzt-1 (**7a**) and pypzt-2 (**7b**).

Results and discussion

Syntheses of the TEMPO-containing ligands

The preparation of the bifunctional molecules is based on the specific chemical properties of 2,4,6-trichloro-1,3,5-triazine (**1**, Scheme 1).[32] The chloride atoms of **1** can be easily and selectively substituted by any nucleophilic reagent.[33] Thus, the temperature controlled substitution of each chloride atom of **1** allows the preparation of triazine derivatives holding up to three different substituents. The synthetic strategy of the investigation herein

reported is therefore to use **1** as a building block to connect on one triazine ring both a ligand aimed at coordinating a Cu^{II} ion and a TEMPO unit which is required for the oxidation reaction to proceed. As is depicted in Scheme 1, the first step of the synthesis is the reaction of **1** with diphenylamine which produces 2,4-dichloro-6-diphenylamino{1,3,5}triazine (**2**) with a yield of 55%.[28] This step is carried out to "neutralize" one of the three chloride positions of the ring as only two functional groups are required for the present study. This position will be used in future investigations to introduce a third functionality. Next, the pyrazole/pyridine ligands possessing a nucleophilic group for their subsequent grafting on the triazine ring are prepared from 2-acetylpyridine (**3**). Reaction of **3** with an excess of *N*,*N*-dimethylformamide dimethyl acetal under reflux generates 3-(dimethylamino)-1-(pyridin-2-yl)prop-2-en-1-one (**4**) with a yield of 40%. The reaction of **4** with 2-hydroxyethyl hydrazine in ethanol at 60 °C produces two pyrazole/pyridine derivatives with a total yield of 83%. These regioisomers **5a** and **5b** can be separated by column chromatography. After deprotonation of the alcoholic function with sodium hydride, each isomer can then react with compound **2** in THF at room temperature to yield **6a** (yield = 85%) and **6b** (yield = 81%), respectively, as crystalline materials. The single-crystal X-ray structures of **6a** and **6b** are depicted in Fig. S1 and S2 (ESI†), respectively. The final step consists of reacting the precursors **6a** and **6b** with 4-amino-TEMPO in THF under reflux during 4 days. This final reaction leads to the targeted bifunctional molecules pypzt-1 (**7a**) and pypzt-2 (**7b**) whose crystal structures are illustrated in Fig. S3 and S4 (ESI†) , respectively.

Catalytic studies

The two TEMPO-containing ligands pypzt-1 and pypzt-2 have been tested in the copper-catalysed aerobic oxidation of two model substrates, *i.e.* benzyl alcohol and 1-octanol. The catalytic reactions were performed applying the experimental conditions described earlier,[25] namely using 5 mol% of $CuBr_2$ together with 5 mol% of the ligand in acetonitrile–water (2 : 1) with potassium *tert*-butoxide as basic co-catalyst. The results are listed in Table 2. The use of pypzt-1 (**7a**) leads to a conversion of 6% after 1 h and 84% after 24 h, while the use of pypzt-2 (**7b**) results in catalytically non-active species (Table 2, entries 1 and 2, respectively). For comparison, the catalytic conversions achieved with the ligands mpypz-1 and mpypz-2 (Scheme 2)[26] have been included in Table 2 (entries 3 and 4). Amazingly,

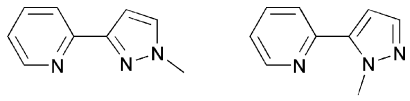

Scheme 2 Ligands related to pypzt-1 and pypzt-2, respectively, used in earlier catalytic studies.[26]

the activities observed are reversed. Indeed, the bidentate ligand mpypz-2 generates an active copper(II) complex, whereas the corresponding ligand pypzt-2 shows no activity (Table 2, entries 4 and 2, respectively). In the same way, the bridging ligand pypzt-1 produces an effective copper catalyst, but not mpypz-1 (Table 2, entries 1 and 3, respectively). In fact, with pypzt-2 (**7b**) a precipitate appears which is not observed with pypzt-1 (**7a**). The same phenomenon was observed with mpypz-2;[26] however, contrary to pypzt-2, the precipitation of copper species does not quench the reaction. Most likely, the insoluble polymeric copper species obtained with mpypz-2 are in equilibrium with soluble, active ones, which is obviously not the case with pypzt-2. The disparities between the activities generated by pypzt-1 and mpypz-1 can be justified by comparable facts. Actually, no precipitation occurs with pypzt-1 while a precipitate is produced with mpypz-1 (for which the catalytic activity is quenched after 1 h of reaction time).[26] It should be noted that the integration of both a pyridine/pyrazole ligand and a TEMPO moiety on a single triazine ring allows the production of a copper catalyst whose activity is equivalent to that achieved with a pyridine/pyrazole ligand and TEMPO added separately (Table 2, entries 1 and 4). The copper catalyst obtained from copper(II) bromide and pypzt-1 is capable of converting 29% of octan-1-ol (an alkyl alcohol whose oxidation is more difficult to achieve) to octanal in 24 h (Table 2, entry 5).

The good solubility of the complex generated from $CuBr_2$ and pypzt-1 in acetonitrile has allowed the preparation of single-crystals of the coordination compound (**8**).

Ligand-field studies

Comparative visible spectroscopy studies of the copper(II) complexes obtained *in situ* from the ligands mpypz-1, mpypz-2, pypzt-1 (**7a**) and pypzt-2 (**7b**) have been carried out (see ESI†for the experimental procedure). The spectra recorded are depicted in Fig. 1. The spectra of 1 : 1 mixtures of Cu–mpypz-1 and Cu–mpypz-2 in acetonitrile show different features (Fig. 1(A)). With mpypz-1, a band at 533 nm and a weaker one at 648 nm are observed. These d–d bands are typical for square-pyramidal Cu^{II}

Table 2 [Copper/TEMPO]-catalysed oxidation of benzyl alcohol and octan-1-ol to the corresponding aldehydes[a]

			Conversion (%)		
Entry	Alcohol	Ligand used	After 1 h	After 24 h	Ref.
1	Benzyl alcohol	pypzt-1	6	84[b]	This work
2	Benzyl alcohol	pypzt-2	—[c]	—[c]	This work
3	Benzyl alcohol	mpypz-1	29[d]	—[c]	26
4	Benzyl alcohol	mpypz-2	8	89	26
5	Octan-1-ol	pypzt-1	6	29	This work

[a] For the reaction procedure, see Experimental Section. [b] A conversion of 93% is reached after a reaction time of 30 hours. [c] No catalytic oxidation was observed. [d] The reaction stops after one hour.[26]

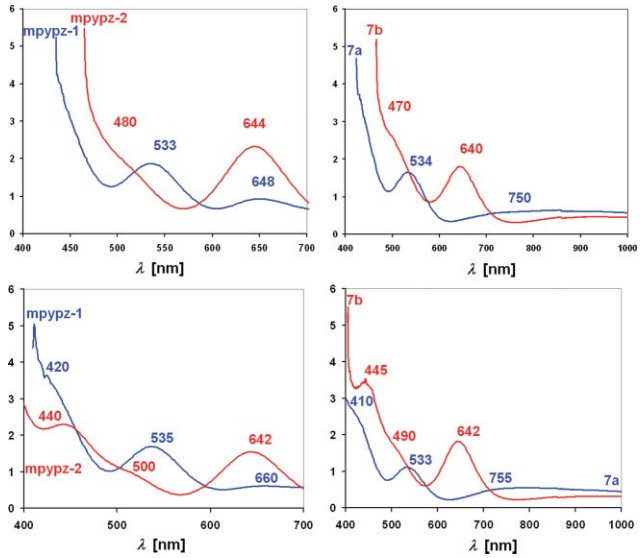

Fig. 1 Electronic spectra for 1 : 1 acetonitrile solutions of Cu–ligand (A and B, top left and right) and for 1 : 1 : 1 acetonitrile solutions of Cu–ligand–base (C and D, bottom left and right).

complexes. For mpypz-2, the bands at 644 nm and around 480 nm also suggest a square-pyramidal coordination environment for the corresponding complex. Comparable spectroscopic characteristics are noticed with the copper(II) compound generated from pypzt-2 (**7b**) (Fig. 1(B)), thus indicating that an analogous coordination geometry. With pypzt-1 (**7a**), two bands are noted at about 750 and 534 nm which may characterize an octahedral geometry. Upon addition of base (Fig. 1(C) and (D)), the spectra for mpypz-1 and **7a** are not altered while changes are observed for mpypz-2 and **7b**. For mpypz-2, an additional weak band is now detected at 500 nm and the initial band at 480 nm is shifted to 440 nm. Similarly, for mpypz-2, three bands are present at 642, 490 and 445 nm.

Electrochemical studies under a variety of conditions resulted in complicated voltammograms showing the involvement of up to five different redox species. The cyclic voltammograms are comparable for all four copper/ligand systems. Spectroelectrochemical investigations would be required to identify these species and are left for a later paper.

Crystal structure

Single-crystals of a complex prepared from pypzt-1 (**7a**) and copper(II) bromide could be obtained. Indeed, the reaction of 1.5 equiv. of $CuBr_2$ with 1 equiv. of pypzt-1 in acetonitrile leads to the formation of orange crystals of $[Cu_2(pypzt\text{-}1)_2Br_3(H_2O)][CuBr_2]\cdot 4CH_3CN$ (**8**) after two days. **8** crystallises in the triclinic space group $P\bar{1}$. An ORTEP view of compound **8** is depicted in Fig. 2. The crystallographic data for the structural analysis and the important bond parameters are listed in Tables S1 and S2 (ESI†), respectively. The dinuclear complex is constituted of two different copper(II) ions characterized by slightly distinct coordination environments (Fig. 2). The Cu1 atom is pentacoordinated and adopts a distorted square-pyramidal arrangement ($\tau_5 = 0.18$).[34] The $Cu^{II}N_3Br_2$ chromophore is formed by a pyrazole N atom and a pyridine N atom from one pypzt-1 ligand, two bromide anions and one N atom from triazine ring belonging to a second pypzt-1 unit. The Cu–N and Cu–Br bond distances

Table 3 Selected bond lengths (Å) and angles (°) for $[Cu_2(\mathbf{L})_2Br_3(H_2O)]^+$ in **8**

Cu1–Br1	2.362(1)	Cu1–Br2	2.687(1)
Cu1–N11	2.111(5)	Cu1–N16	2.011(5)
Cu1–N53	2.066(5)	Cu1–O57	2.864(5)
Cu2–Br3	2.357(1)	Cu2–O100	2.400(4)
Cu2–N61	2.052(6)	Cu2–N66	2.021(7)
Cu2–N3	2.007(5)	Cu2–O7	2.792(5)
Br1–Cu1–Br2	93.39(3)	Br1–Cu1–N11	101.71(14)
Br1–Cu1–N16	178.67(15)	Br1–Cu1–N53	89.90(14)
Br2–Cu1–N11	106.96(15)	Br2–Cu1–N16	85.30(14)
Br2–Cu1–N53	113.29(14)	N11–Cu1–N16	78.5(2)
N11–Cu1–N53	137.3(2)	N16–Cu1–N53	90.8(2)
Br3–Cu2–O100	86.27(12)	Br3–Cu2–N61	103.38(19)
Br3–Cu2–N66	167.59(19)	Br3–Cu2–N3	92.32(16)
O100–Cu2–N61	109.5(2)	O100–Cu2–N66	81.4(2)
O100–Cu2–N3	106.47(19)	N61–Cu2–N66	80.1(3)
N61–Cu2–N3	141.4(2)	N66–Cu2–N3	92.1(2)

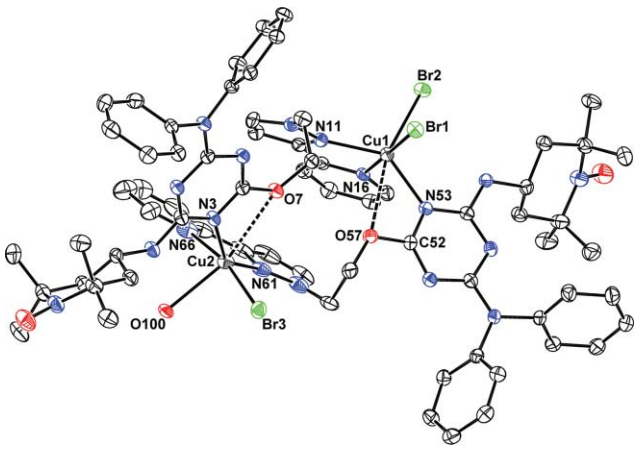

Fig. 2 ORTEP drawing of the cationic part of compound **8**. Thermal ellipsoids are drawn at the 30% probability level. H atoms, lattice solvent molecules and non-coordinated anions are not shown for clarity.

(Table 3) are typical for such coordination geometry.[35] The basal angles varying from 78.4(2) to 101.72(17)° reflect the distortion which is most likely due to steric hindrance resulting from the coordination of the triazine ring of the adjacent ligand (nitrogen atom N53; Fig. 2). In addition, the oxygen atom O57 of this pypzt-1 ligand is semi-coordinated to Cu1 (Cu1–O57 2.864(5) Å), giving rise to a constrained four-membered coordination unit (including the atoms Cu1, N53, C52 and O57; Fig. 2). The coordination geometry around Cu2 is analogous to that of Cu1. Like Cu1, Cu2 is coordinated by a pyrazole/pyridine unit and triazine nitrogen atom. The coordination sphere of the metal centre is completed by a bromide anion and a water molecule (Fig. 2). The τ_5 value for Cu2 is 0.19,[34] characterizing a distorted square-pyramidal geometry. The Cu–N, Cu–Br and Cu–O bond lengths of the $Cu^{II}N_3BrO$ chromophore are in normal ranges.[36] The distortion is due to the coordination of the triazine ring, which generates steric constraints enhanced by the semi-coordination of the oxygen atom O7 (Cu2–O7 2.792(5) Å; Fig. 2). Furthermore, the axial water molecule (oxygen atom O100) is hydrogen bonded to the amine nitrogen atom N21 (N21 ⋯ O100 3.050(8), N21–H21–O100 175°; Fig. 2).

The crystal lattice of **8** reveals interesting features. First, $[Cu^{I}Br_2]^-$ anions are present (Fig. 3). The formation of these

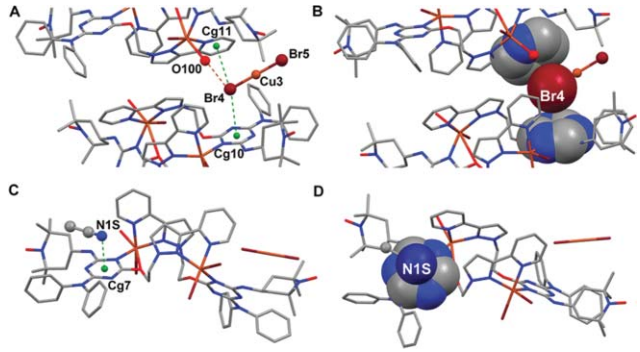

Fig. 3 Illustrations showing a lattice $[CuBr_2]^-$ anion and its hydrogen bonding and anion–π interactions (A, B), and acetonitrile lone pair–triazine ring interactions (C, D).

uncommon copper(I) dibromide ions[37,38] is most likely mediated by the Cu^{II}/TEMPO system, thus revealing its redox properties.

The $[Cu^{I}Br_2]^-$ anions appear to be stabilised by means of supramolecular interactions (Fig. 3(A) and (B)). Indeed, the bromide atom Br4 of the copper(I) dibromide unit is in contact with two heteroaromatic rings (labelled as Cg10 and Cg11 in Fig. 3(A)). These anion–π interactions[39,40] are characterised by anion–centroid distances of 3.691(3) Å (Cg10 · · · Br4) and 3.781(5) Å (Cg11 · · · Br4) and [Br4 axis–ring centroid–ring plane] angles of 82.78(3)° (Cg10) and 85.65(3)° (Cg11) (see Table S3 (ESI†) for all [ring atom] · · · Br4 contact distances). In addition, the bromide atom Br4 is hydrogen-bonded to the water molecule coordinated to Cu2 (the distance O100–H1w · · · Br5 of 3.377(5) Å and the O100–H1w–Br5 angle of 138° characterise a moderate hydrogen bonding interaction[41]).

As is evidenced in Fig. 2, **8** contains two pypzt-1 ligands and therefore two electron-deficient triazine rings. As mentioned above, the triazine unit Cg10 (Fig. 3(A)) is involved in anion–π interactions. Amazingly, the second triazine ring, labelled Cg7 (Fig. 3(C)), is in contact with the nitrogen atom N1S of a lattice acetonitrile molecule. Such remarkable lone pair–aromatic interactions[42] has been previously observed in the crystal structure of a zinc(II) complex.[43] The present $(\text{lone pair})_{\text{acetonitrile}}$–$\pi_{\text{triazine}}$ interaction is characterized by a N1S · · · Cg7 distance of 3.348(11) Å and a [N1S axis–ring centroid–ring plane] angle of 80.16(2)° (see Table S4 (ESI†) for all [ring atom] · · · N1S contact distances).

Physical properties of complex 8

The magnetic properties of **8** have been investigated in some detail. The $\chi_M T$ and χ_M *vs.* T plots (χ_M is the molar magnetic susceptibility) are shown in Fig. 4. At room temperature, $\chi_M T$ is *ca.* 1.55 $cm^3\ mol^{-1}$ K, being consistent with the expected value for four non-interacting $S = 1/2$ centers (1.5 cm^3 K mol^{-1} for $g = 2$). These results show that no interactions between the copper centres and the TEMPO units are occurring. Upon cooling $\chi_M T$ remains constant until 60 K where it starts to decrease, illustrating an antiferromagnetic behaviour. To estimate the magnitude of the antiferromagnetic coupling, the magnetic susceptibility data were fitted to the Curie–Weiss law for four interacting $S = 1/2$ centers (two Cu^{II} ions and two TEMPO radicals). The fitting of the data gives $g = 1.97$, $\theta = -3.52$ K and $R = 2 \times 10^{-4}$; R symbolizes the agreement factor defined as $\sum_i(\chi_{calc} - \chi_{obs})^2/\sum_i(\chi_{obs})^2$.

The solid line in Fig. 4 corresponds to the theoretical curve obtained using the above parameters. The poor Curie–Weiss fit for **8** is indicative of a probable intermolecular antiferromagnetic super-exchange pathway in this compound. When cooled, the χ_M value increases continuously, from 7.46×10^{-3} $cm^3\ mol^{-1}$ at 300 K, to reach a value of 0.46 $cm^3\ mol^{-1}$ below 2 K. This behaviour typically points towards the occurrence of weak antiferromagnetic interactions at low temperatures.

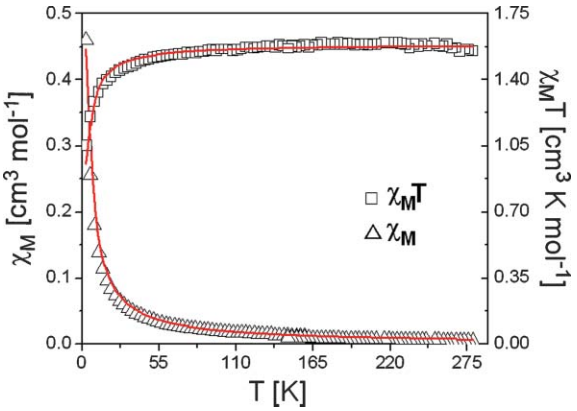

Fig. 4 Plots of $\chi_M T$ *vs.* T (□) and χ_M *vs.* T (△) for **8**. The solid lines are a fit to the experimental data (see text).

The EPR spectrum of an acetonitrile solution of complex **8** at room temperature shows a broad signal centered at $g = 2.054$ and a three-line signal with $g = 2.003$ and $A\{^{14}N\} = 16$ G (Fig. 5). No half-field signal was detected. The three-line signal characterises non-interacting TEMPO moieties.[44] In the strong exchange limit for Cu^{II}/nitroxyl radical coupling, the g value for a coordination compound including copper(II) and n spin-labelled units ($L^{\bullet}$) can be estimated using eqn (1).[45]

$$g_{obs} = (ng_{L^{\bullet}} + g_{Cu})/(n + 1) \quad (1)$$

For five-coordinated $Cu^{II}N_3Br_2$ and $Cu^{II}N_3BrO$ chromophores, g values from 2.10 to 2.15 are expected.[35,36] Compound **8** exhibits one TEMPO unit per copper(II) ion; therefore, the calculated g_{obs} value is in the range 2.051–2.076. The experimental value of 2.054

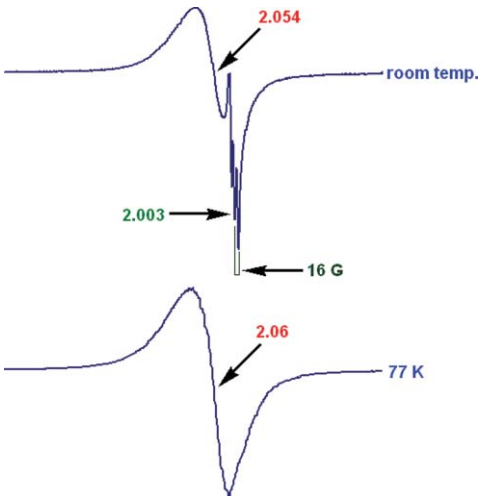

Fig. 5 EPR spectra of complex **8** in acetonitrile solution at room temperature (top) and at 77 K (bottom).

is in good agreement as it is in the expected range. At 77 K, the three-line signal disappears (Fig. 5) which suggests the occurrence of intermolecular Cu^{II}/TEMPO interactions in the lattice. The broad signal observed is centered at $g = 2.06$, which is consistent with the range value obtained from eqn (1).

In the presence of base, the broad signal corresponding to the copper(II) species ($g = 2.054$) disappears which suggests the formation of dinuclear species.

Concluding remarks

A new 1,3,5-triazine derivative has been designed to contain both a binding site for copper(II) ions and a TEMPO sub-unit. The objective was to obtain a Cu^{II}/TEMPO complex able to catalyse a two-electron oxidation process, namely the oxidation of a primary alcohol to the corresponding aldehyde (galactose oxidase activity). Actually, the copper(II) complex obtained by the coordination of Cu^{II} ions to the bifunctional ligand pypzt-1 is able to convert (as anticipated) benzyl alcohol and octan-1-ol to the aldehydic products, under mild conditions in air. Moreover, the catalytic activity observed is analogous to that achieved when a related ligand (mpypz-2)[26] and TEMPO are added as single molecules to the reaction mixture. Therefore, the incorporation of both the copper unit and the TEMPO group on a single molecule does not reduce the catalytic activity. Interestingly, the crystal lattice of complex **8** reveals the presence of unusual $[Cu^{I}Br_2]^-$ anions which are involved in hydrogen-bonding and anion–π interactions. In addition, the solid-state X-ray structure of **8** exhibits only the second crystallographic evidence of acetonitrile (lone pair)–triazine (electron-deficient ring) interactions.

New molecules with different spacer lengths between the different functional units (ligand or TEMPO moiety) and the triazine ring are currently investigated. It is expected that an optimal spacer length will enhance the catalytic activity of the resulting TEMPO ligand. Indeed, in the present system, the short length of the spacer connecting the TEMPO unit to the triazine ring prevents its intramolecular interaction with the copper centre. Moreover, the third position is now used to anchor the copper/TEMPO catalyst on a solid support.

Acknowledgements

The investigations described in this paper were supported by the Graduate Research School Combination "NRSC Catalysis", a joint activity of the graduate research schools NIOK, HRSMC and PTN. The COST program Action D35/0011 is also kindly acknowledged.

References

1 R. A. Sheldon, *J. Chem. Technol. Biotechnol.*, 1997, **68**, 381–388.
2 S. S. Stahl, *Angew. Chem., Int. Ed.*, 2004, **43**, 3400–3420.
3 S. S. Stahl, *Science*, 2005, **309**, 1824–1826.
4 J. March, *Advance Organic Chemistry; Reaction, Mechanisms and Structure*, John Wiley & Sons, New York, 4th edn, 1992.
5 *Organic Syntheses by Oxidation with Metal Compounds*, Plenum, New York, 1986.
6 R. A. Sheldon, I. W. C. E. Arends, G. J. Ten Brink and A. Dijksman, *Acc. Chem. Res.*, 2002, **35**, 774–781.
7 T. Mallat and A. Baiker, *Chem. Rev.*, 2004, **104**, 3037–3058.
8 C. Lin, C. Z. Xu, C. G. Xia and Y. H. Feng, *Prog. Chem.*, 2004, **16**, 758–765.
9 P. J. Figiel, M. Leskela and T. Repo, *Adv. Synth. Catal.*, 2007, **349**, 1173–1179.
10 D. Geisslmeier, W. G. Jary and H. Falk, *Monatsh. Chem.*, 2005, **136**, 1591–1599.
11 X. F. Zhao and C. Zhang, *Synthesis*, 2007, 551–557.
12 N. Jiang and A. J. Ragauskas, *J. Org. Chem.*, 2006, **71**, 7087–7090.
13 C. Bolm, A. S. Magnus and J. P. Hildebrand, *Org. Lett.*, 2000, **2**, 1173–1175.
14 I. A. Ansari and R. Gree, *Org. Lett.*, 2002, **4**, 1507–1509.
15 W. Adam, C. R. Saha-Moller and P. A. Ganeshpure, *Chem. Rev.*, 2001, **101**, 3499–3548.
16 S. Mannam, S. K. Alamsetti and G. Sekar, *Adv. Synth. Catal.*, 2007, **349**, 2253–2258.
17 S. Striegler, *Tetrahedron*, 2006, **62**, 9109–9114.
18 R. A. Sheldon and I. W. C. E. Arends, *J. Mol. Catal. A: Chem.*, 2006, **251**, 200–214.
19 S. Velusamy, A. Srinivasan and T. Punniyamurthy, *Tetrahedron Lett.*, 2006, **47**, 923–926.
20 M. Contel, C. Izuel, M. Laguna, P. R. Villuendas, P. J. Alonso and R. H. Fish, *Chem. Eur. J.*, 2003, **9**, 4168–4178.
21 G. Ragagnin, B. Betzemeier, S. Quici and P. Knochel, *Tetrahedron*, 2002, **58**, 3985–3991.
22 B. Betzemeier, M. Cavazzini, S. Quici and P. Knochel, *Tetrahedron Lett.*, 2000, **41**, 4343–4346.
23 N. Tsubokawa, T. Kimoto and T. Endo, *J. Mol. Catal. A: Chem.*, 1995, **101**, 45–50.
24 P. Gamez, I. W. C. E. Arends, R. A. Sheldon and J. Reedijk, *Adv. Synth. Catal.*, 2004, **346**, 805–811.
25 P. Gamez, I. W. C. E. Arends, J. Reedijk and R. A. Sheldon, *Chem. Commun.*, 2003, 2414–2415.
26 J. S. Uber, Y. Vogels, D. Van Den Helder, I. Mutikainen, U. Turpeinen, W. T. Fu, O. Roubeau, P. Gamez and J. Reedijk, *Eur. J. Inorg. Chem.*, 2007, 4197–4206.
27 O. Kahn, *Molecular Magnetism*, VCH Publishers, New York, 1993.
28 Z. L. Lu, P. Gamez, I. Mutikainen, U. Turpeinen and J. Reedijk, *Cryst. Growth Des.*, 2007, **7**, 1669–1671.
29 P. Gamez, R. H. Steensma, W. L. Driessen and J. Reedijk, *Inorg. Chim. Acta*, 2002, **333**, 51–56.
30 G. M. Sheldrick, *SHELXS-97 Program for Crystal Structure Determination*, University of Göttingen, Germany, 1997.
31 G. M. Sheldrick, *SHELXL-97-2 Program for Crystal Structure Refinement*, University of Göttingen, Germany, 1997.
32 P. de Hoog, P. Gamez, W. L. Driessen and J. Reedijk, *Tetrahedron Lett.*, 2002, **43**, 6783–6786.
33 P. Gamez and J. Reedijk, *Eur. J. Inorg. Chem.*, 2006, 29–42.
34 A. W. Addison, T. N. Rao, J. Reedijk, J. van Rijn and G. C. Verschoor, *J. Chem. Soc., Dalton Trans.*, 1984, 1349–1356.
35 J. Carranza, J. Sletten, C. Brennan, F. Lloret, J. Cano and M. Julve, *Dalton Trans.*, 2004, 3997–4005.
36 Y. Mikata, T. Fujimoto, Y. Sugai and S. Yano, *Eur. J. Inorg. Chem.*, 2007, 1143–1149.
37 W. B. Kim and J. S. Lee, *J. Phys. Chem. B*, 2003, **107**, 9195–9202.
38 P. C. Healy, L. M. Engelhardt, V. A. Patrick and A. H. White, *J. Chem. Soc., Dalton Trans.*, 1985, 2541–2545.
39 P. Gamez, T. J. Mooibroek, S. J. Teat and J. Reedijk, *Acc. Chem. Res.*, 2007, **40**, 435–444.
40 B. L. Schottel, H. T. Chifotides and K. R. Dunbar, *Chem. Soc. Rev.*, 2008, **37**, 68–83.
41 J. W. Steed and J. L. Atwood, *Supramolecular Chemistry*, John Wiley & Sons, Ltd, Chichester, New York, Weinheim, Brisbane, Singapore, Toronto, 2000.
42 M. Egli and S. Sarkhel, *Acc. Chem. Res.*, 2007, **40**, 197–205.
43 T. J. Mooibroek, S. J. Teat, C. Massera, P. Gamez and J. Reedijk, *Cryst. Growth Des.*, 2006, **6**, 1569–1574.
44 M. A. Halcrow, L. M. Rodriguez-Martinez, E. K. Brechin, J. E. Davies, I. J. Scowen and M. McPartlin, *J. Organomet. Chem.*, 1999, **573**, 171–179.
45 S. S. Eaton and G. R. Eaton, *Coord. Chem. Rev.*, 1988, **83**, 29–72.